Quantum-clustered two-photon walks

David S. Simon, Shuto Osawa, and Alexander V. Sergienko

Quantum-Clustered Two-Photon Walks

David S. Simon,[1, 2, *] Shuto Osawa,[2, †] and Alexander V. Sergienko[2, 3, ‡]

[1]*Dept. of Physics and Astronomy, Stonehill College, 320 Washington Street, Easton, MA 02357*
[2]*Dept. of Electrical and Computer Engineering & Photonics Center,*
Boston University, 8 Saint Mary's St., Boston, MA 02215, USA
[3]*Dept. of Physics, Boston University, 590 Commonwealth Ave., Boston, MA 02215, USA*

We demonstrate a previously unknown two-photon effect in a discrete-time quantum walk. Two identical bosons with no mutual interactions nonetheless can remain clustered together as they walk on a lattice of *directionally-reversible* optical four-ports acting as Grover coins; both photons move in the *same* direction at each step due to a two-photon quantum interference phenomenon reminiscent of the Hong-Ou-Mandel effect. The clustered two-photon amplitude splits into two localized parts, one oscillating near the initial point, and the other moving ballistically without spatial spread, in soliton-like fashion. But the two photons are always clustered in the *same* part of the superposition, leading to potential applications for transport of entanglement and opportunities for novel two-photon interferometry experiments.

I. INTRODUCTION

The Hong-Ou-Mandel (HOM) effect [1] is probably the best known two-photon interference effect. Two identical photons are simultaneously incident on different inputs of a 50/50 beam splitter (BS) as in Fig. 1(a). Each photon could exit either output port, so naively one expects nonzero amplitudes for three possible outcomes: both exiting at port 3, both exiting at port 4, or one photon each at ports 3 and 4. But in fact, no coincidences are seen between 3 and 4; the two photons always leave at the same port. *Which* port the pair exits is entirely random. Coincidences between the two output ports are absent because of cancelations between the two indistinguishable processes on the upper line of Fig. 1(b). As a result, the two photons always remain clustered together in the same output spatial mode. This gives a method for measuring time intervals to sub-picosecond level accuracy: as a delay between the photons varies, the coincidence rate exhibits a sharp dip (the HOM dip) when the wavefunctions briefly overlap on the BS.

Quantum walks [5, 6] are currently a subject of extensive investigation, in part because they have been shown to be formally equivalent to a universal quantum computer [2–4], and so they provide new insights into a variety of quantum algorithms, especially quantum search algorithms. In a Hadamard walk, the walker's amplitude produces two peaks that move ballistically in opposite directions (Fig. 2(a)), so the distribution's width grows linearly in time, $\sigma \sim t$. In contrast, classical random walks give approximately Gaussian distributions whose widths spread diffusively ($\sigma \sim \sqrt{t}$). Consequently, quantum walks can probe large regions faster than classical walks, leading to quantum speedups of walk-based algorithms. Details differ for specific implementations of quantum walks, but discussion of quadratic speedups can be found in [7] for Hadamard walks and in [8, 9] for Grover walk-based searches.

A variety of two-particle quantum walks have been studied [10–19]. Here we look at a novel arrangement in which two indistinguishable bosons undergo a discrete-time quantum walk along a dual rail or ladder type system (Fig. 3(a)), with a four-dimensional Grover coin at each vertex. Such a chain could be considered as a pair of quantum wires (representing a pair of states), with the Grover coins serving as directional couplers [20, 21] between them; more pertinently to our purposes here, we may also think of the system as a single double-stranded quantum wire in which we care only about the horizontal location of the particle, not whether it is on the upper or lower strand.

For specificity, assume that the walking particles are photons. Then the Grover coins can be implemented using a linear-optical four-port (Fig. 4), which is a special case of the directionally-unbiased multiports studied in
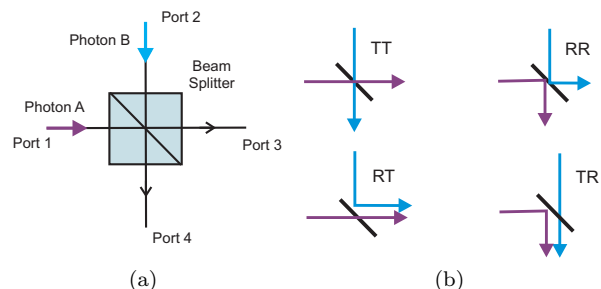

FIG. 1: Two photons entering a beam splitter at different ports (a) lead to four different outcomes (b), labeled according to whether each photon reflects (R) or transmits (T). Outcomes on the top line (RR and TT) are indistinguishable. Being of equal magnitude but opposite sign, their amplitudes cancel, so coincidences between output ports vanish. Although exiting at a random output port, both photons are always found to cluster together in the *same* port.

[*]e-mail: `simond@bu.edu`
[†]e-mail: `sosawa@bu.edu`
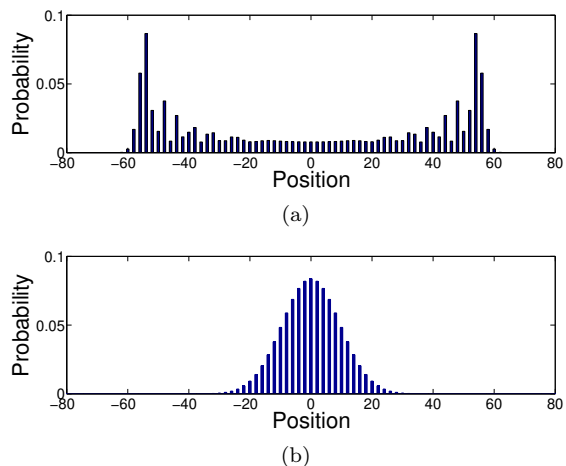[‡]e-mail: `alexserg@bu.edu`

FIG. 2: (a) Typical 1-dimensional (Hadamard) quantum walk. Spatial probability distributions have low probability of remaining near the origin and widths that grow linearly with time. (b) In contrast, classical walks yield approximately Gaussian distributions, whose widths grow more slowly, $\sim \sqrt{t}$.
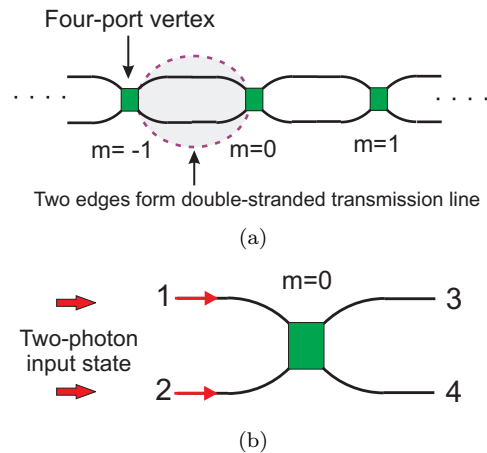

FIG. 3: (a) A chain of four-ports connected by pairs of edges. Each edge pair is thought of as a single double-stranded connection line, and vertex positions are labeled by integers. (b) The initial state consists of two indistinguishable, right-moving photons injected into ports 1 and 2 of the $m = 0$ multiport, in the middle of the chain.

[22–27]. The three-port version of this device has been demonstrated in a tabletop set-up [26], and initial work on integrated chip versions of such structures is underway. The system is based entirely on linear optics, with no interactions between the photons. In particular, if the photons are *distinguishable*, then each exhibits an independent quantum walk and can later be detected in widely separated spatial regions. However, once the photons become *indistinguishable*, the two-photon interference alters the picture: it is shown below that for a particular input state the two photons remain spatially clustered and are always found at the *same* horizontal location at each moment. Moreover, the two-photon amplitude shows no sign of the randomness normally associated with random walks: it splits into a quantum superposition of two localized packets that each move deterministically over time with the two photons always remaining clustered in one packet or the other.

These effects depend only on indistinguishable photons being inserted into the same Grover coin vertex simultaneously; entanglement is not required. However, if the photons *are* entangled then they remain together with entanglement undiminished as they move, opening up new possibilities for quantum information processing, as briefly commented upon in the conclusion.

Experimentally, the most practical realization of the structures described here are on integrated optical chips. Losses, decoherence, and chip imperfections will of course limit the possible walk lengths of experimental implementations. Up to this point, quantum walks of both single photons and of entangled photon pairs have typically been implemented using integrated optics for walks of lengths on the order of five to ten time steps (for example, [15, 28–30]), although proposals have been made

for arrangements that may allow longer walks [31]. In what follows, we assume an idealized system, neglecting losses and other imperfections.

II. SETUP AND MAIN RESULT.

Consider a directionally-unbiased four-port acting as a Grover coin [32, 33], with ports labeled as in Fig. 3(b). The action of the four-port is given by the unitary matrix

$$U = \frac{1}{2} \begin{pmatrix} -1 & 1 & 1 & 1 \\ 1 & -1 & 1 & 1 \\ 1 & 1 & -1 & 1 \\ 1 & 1 & 1 & -1 \end{pmatrix}, \tag{1}$$

where rows and columns represent the four ports. Regardless of which port a photon enters, exit amplitudes at all outputs are real and equal in magnitude. Importantly, the amplitude to reflect back to the input port has an extra minus sign relative to all other transitions.

Consider two photons entering the linear chain of Fig. 3(a) simultaneously. Assume one enters port 1 and the other enters port 2 of the same multiport, as in Fig. 3(b), somewhere in the middle of the chain, far enough from the ends that we don't need to worry about the photons leaving the system during the time duration of the experiment. Experimentally, two photons can be produced simultaneously using spontaneous parametric down conversion [34] and then coupled into the chain by means of an electro-optical or magneto-optical switch. Horizontal positions are specified by an integer m corresponding to the multiport label, and discrete time $t = nT$ by integer n, where T is the photon travel time between multiports.
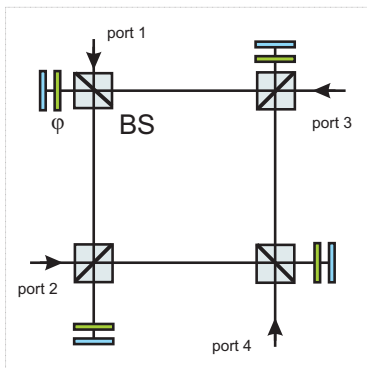
FIG. 4: One possible optical implementation of the four-dimensional Grover coin, the directionally-reversible four-port device. Photons can both enter and exit each of the four external ports. At each corner of the loop there is a beam splitter, a mirror (green) and a phase shifter (blue). Similar n-port devices can be constructed for any n; their workings are analyzed in details in [22] and the three-port version is experimentally demonstrated in [26].

At time $n = 0$, the photons are moving rightward, entering the $m = 0$ multiport.

Then if the locations of the two photons at any later time $n > 0$ are measured, two striking things are found. First, the photons cluster spatially: if the two parallel input/output edges between adjacent multiports are treated as a single double-stranded connecting line, then the photons are always found on the *same* double line. Assuming no loss and ideal measuring devices, measurement at any horizontal location always finds either two photons or none. This can be seen as a quantum walk analog of the HOM effect: amplitudes for indistinguishable outcomes in which the photons move apart always cancel among themselves, as will be shown in the next section. However, the HOM quantum interference effect occurs just once, whereas clustering of the walk persists indefinitely, over an arbitrarily long sequence of steps.

Second, this clustered two-photon amplitude behaves in an unusual manner. It breaks after the first step into a *sustainable superposition of two distinct localized states* (Fig. 5). One two-photon cluster in the superposition moves away from the starting point ballistically, exhibiting no randomness. The other cluster stays near $m = 0$, bouncing back and forth between two adjacent locations (a phenomenon dubbed oscillatory localization [35]). So another way to look at the state is as an odd sort of two-photon clustered Schrodinger cat state, in which the parts of the cat rapidly separate from each other: the two-photon cat speeds away after a rat *and* simultaneously remains rocking contentedly in its warm cat bed.

For comparison, imagine a *single* photon entering the present system, initially localized on one input port. This can be seen as the sum of two states: one symmetric over
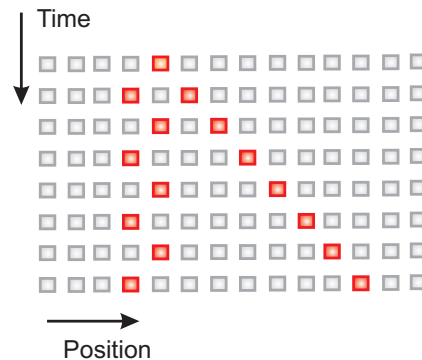

FIG. 5: After the first step, the amplitude splits: it becomes an equal superposition of two photons moving away ballistically, and two photons oscillating near the initial point.

the upper and lower lines and one antisymmetric,

$$|1\rangle = \frac{1}{2}(|1\rangle + |2\rangle) + \frac{1}{2}(|1\rangle - |2\rangle) \qquad (2)$$
$$= |\psi_s\rangle + |\psi_a\rangle. \qquad (3)$$

The symmetric part will always continue rightward at each step, while the antisymmetric portion reflects at each step, leading to oscillations. These single-particle behaviors have been previously discussed in [35] for Grover coin systems. What is remarkable in the two-particle case is that measurement of the two particles will always find them in the *same* part of the superposition; one will never be found in the oscillating portion and the other in the ballistic portion. Which part of the superposition the two photons are found to be clustered in is completely random, just as the output port in which the two photons are clustered in the HOM effect is purely random.

The two halves of the clustered amplitude do not spread as they propagate, exhibiting soliton-like behavior. Note that the wavepacket spread in quantum walks is of statistical origin, not a result of dispersive material properties. So cancelation of spreading occurs in the current system from linear interference processes, with no need for nonlinear interactions.

III. TIME EVOLUTION

A. First time step

Here we sketch the time evolution of the system. Additional details of the calculations can be found in Appendix A.

Momentarily treating the photons as distinguishable, there are 16 possible exit outcomes from the four-port for the input state of Fig. 3(b). Applying tensor product $U \otimes U$ to the two-photon input, each of these real exit amplitudes has absolute value $\left(\frac{1}{2}\right)^2 = \frac{1}{4}$ if the photons exit at *different* ports, or $\frac{\sqrt{2}}{4} = \frac{1}{2\sqrt{2}}$ if they exit at

the *same* port. (The extra $\sqrt{2}$ appears when the indistinguishability is restored, due to the normalization of two-boson Fock states, $|2\rangle = \frac{1}{\sqrt{2}}\left(a^\dagger\right)^2|0\rangle$.) Amplitudes gain one minus sign for each photon that exits back out the port through which it entered. So signs and magnitudes of all transition amplitudes are readily obtained; these are tabulated in the Appendix.

The initial state is $|\psi_0\rangle_{in} = |12; 0, RR\rangle$; the notation $|ij; m, RR\rangle$ (or $|ij; m, LL\rangle$) means one right-moving (left-moving) photon in port i and one in port j at lattice site m. The resulting output state is

$$|\psi_1\rangle = \frac{1}{2\sqrt{2}}\left[|33; 0, RR\rangle + |44; 0, RR\rangle - |11; 0, LL\rangle \right. \quad (4)$$
$$\left. -|22; 0, LL\rangle\right] + \frac{1}{2}\left[|34; 0, RR\rangle + |12; 0, LL\rangle\right].$$

Assume we only want to know the exit direction of the photons (left or right), and don't care if the photon is in the upper or lower channel. Then, clustering can already be seen in the transition probabilities for the first step of the walk:

• One possible outcome is for both photons entering the left side of the multiport to exit back on the left side ($LL \to LL$). The probability of this is the sum of three terms corresponding respectively to the amplitudes of both photons exiting at port 1, one photon at each port, and both at port 2:

$$P(LL \to LL) = P(|12\rangle \to |11\rangle) + P(|12\rangle \to |12\rangle)$$
$$+P(|12\rangle \to |22\rangle) \quad (5)$$
$$= \left(-\frac{1}{2\sqrt{2}}\right)^2 + \left(\frac{1}{2}\right)^2 + \left(-\frac{1}{2\sqrt{2}}\right)^2$$
$$= \frac{1}{2}. \quad (6)$$

• Similarly, both photons can exit right (ports 3 and 4):

$$P(LL \to RR) = P(|12\rangle \to |33\rangle) + P(|12\rangle \to |34\rangle)$$
$$+P(|12\rangle \to |44\rangle) \quad (7)$$
$$= \left(+\frac{1}{2\sqrt{2}}\right)^2 + \left(\frac{1}{2}\right)^2 + \left(\frac{1}{2\sqrt{2}}\right)^2$$
$$= \frac{1}{2}. \quad (8)$$

• Finally, one photon can exit left and one right. The appearance of extra minus signs in half the amplitudes (see Appendix A) leads to complete cancelation:

$$P(LL \to LR) = P(12 \to 13) + P(12 \to 14) \quad (9)$$
$$+P(12 \to 23) + P(12 \to 24)$$
$$= 0. \quad (10)$$

The result is that *even though the photons do not interact and should walk independently, they in fact always step in the same direction: both go right or both go left.* Destructive interference between indistinguishable amplitudes conspires to eliminate outcomes in which they step in opposite directions.

B. Subsequent steps

The paragraphs above describe the first step. Transition amplitudes can again be tabulated to find the outcomes of subsequent steps. Summing over unmeasured intermediate states in previous steps, one finds the amplitude splitting into an equal superposition of two two-photon states.

The output of the first step (Eq. 4) can be written as

$$|\psi_1\rangle_{out} = \frac{1}{\sqrt{2}}\left(|\psi_t; 0, RR\rangle + |\psi_r; 0, LL\rangle\right), \quad (11)$$

where

$$|\psi_t; m, R\rangle = \frac{|33; m, RR\rangle + |44; m, RR\rangle}{2} \quad (12)$$
$$+\frac{|34; m, RR\rangle}{\sqrt{2}}$$
$$= \frac{|11; m+1, RR\rangle + |22; m+1, RR\rangle}{2} \quad (13)$$
$$+\frac{|12; m+1, RR\rangle}{\sqrt{2}}$$
$$|\psi_r; m, LL\rangle = -\frac{|11; m, LL\rangle + |22; m, LL\rangle}{2} \quad (14)$$
$$+\frac{|12; m, LL\rangle}{\sqrt{2}}$$
$$= -\frac{|33; m-1, LL\rangle + |44; m-1, LL\rangle}{2} \quad (15)$$
$$+\frac{|34; m-1, LL\rangle}{\sqrt{2}}.$$

Here, we used the fact that states leaving ports 3 and 4 enter the adjacent vertex at ports 1 and 2, respectively.

Suppressing some labels for brevity, one finds that applying $U \times U$ again gives

$$\frac{|11\rangle + |22\rangle}{2} \to \frac{|33\rangle + |44\rangle + |11\rangle + |22\rangle}{4} + \frac{|34\rangle - |12\rangle}{2\sqrt{2}} \quad (16)$$
$$\frac{|12\rangle}{\sqrt{2}} \to \frac{|33\rangle + |44\rangle - |11\rangle - |22\rangle}{4} + \frac{|34\rangle + |12\rangle}{2\sqrt{2}}. \quad (17)$$

Taking the sum of these as in Eq. 13, one finds that the amplitudes $|11\rangle$, $|22\rangle$, and $|12\rangle$ cancel out at each step, so that $|\psi_t\rangle$ simply reproduces itself, but shifted one step to the right:

$$|\psi_t; m, RR\rangle \to |\psi_t; m+1, RR\rangle \to |\psi_t; m+2, RR\rangle \to \dots. \quad (18)$$

This is the *ballistic* state: it is *totally transmitting* at each step. If the initiating state of the walk had been moving left ($|34; m, LL\rangle$ instead of $|12; m, RR\rangle$), similar ballistic motion occurs to the left.

The multiport action on $|\psi_r\rangle$ of Eq. 14 is found by taking the difference of Eqs. 16 and 17, leading to cancellation of $|33\rangle$, $|44\rangle$, and $|34\rangle$ terms. So $|\psi_r; m, RR\rangle$ simply reflects at each multiport encounter, causing it to bounce back and forth indefinitely:

$$|\psi_r; m, RR\rangle \to |\psi_r; m-1, LL\rangle \to |\psi_r; m, RR\rangle \to \dots \quad (19)$$

The state is *totally reflecting* at each step, and the amplitude acts as if it is confined in a virtual cavity, oscillating between lattice sites $m = 0$ and $m = 1$.

Up to a spatial shift of one step per unit time, the states $|\psi_t\rangle$ and $|\psi_r\rangle$ are both eigenstates of $(U \times U)^2$, with eigenvalue $+1$, so evolution on subsequent steps is simply a repetition of what happened in the first two steps: one two-photon amplitude repeatedly reflects, the other repeatedly transmits.

So the photons remain spatially clustered as they walk along the line. This quantum walk-based analog of the HOM effect might be referred to as a *quantum-clustered two-photon walk*. But in addition, the two-photon state at each moment localizes onto a quantum superposition of just two nondispersive spatial amplitudes: one moves ballistically at constant speed, while the other flips direction at each step and never moves more than one unit from its starting point. This is analogous to the single-particle Grover walk behavior, but with the unexpected feature that the two photons are always found clustered in the same localized part of the distribution and never separate from each other.

The behavior of the system is shown in Fig. 6, where the amplitude for the position of each photon is shown. It is clearly seen that the amplitude splits into two localized portions, with one portion staying near the origin and the other moving away at constant speed. Moreover, it can be seen that the two indistinguishable photons remain together: there is no amplitude away from the diagonal. In contrast, if the two photons are distinguishable (Fig. 7), the lack of destructive interference leads to the appearance of nonzero off-diagonal amplitudes, indicating that the photons may become spatially separated.

In all of the considerations above, the two photons were assumed to be in a product states. In the next section, we examine the behavior of polarization entangled states in this system.

IV. POLARIZATION-ENTANGLED INPUT

Up to now, no entanglement has been assumed between the two input photon states. Now suppose that the two photons inserted at the origin are polarization-entangled. In particular, define the states:

$$|A_\pm^{ij}\rangle = \frac{1}{\sqrt{2}} \{|iH\rangle|jV\rangle \pm |iV\rangle|jH\rangle\} \qquad (20)$$

$$|B_\pm^{ij}\rangle = \frac{1}{\sqrt{2}} \{|iH\rangle|iV\rangle \pm |jV\rangle|jH\rangle\} \qquad (21)$$

Here, i, j label the input/outport ports, while H and V label polarization states at each port. When necessary, we can add position and direction labels, for example $|A_\pm^{ij}, m, LL\rangle$ or $|B_\pm^{ij}, m, LR\rangle$. These states are polarization-entangled for $i \neq j$. For $i = j$, the $+$ states are product states, while the $-$ states vanish. It is straightforward to work out the action of the multiport on these states by the same means as in section III.
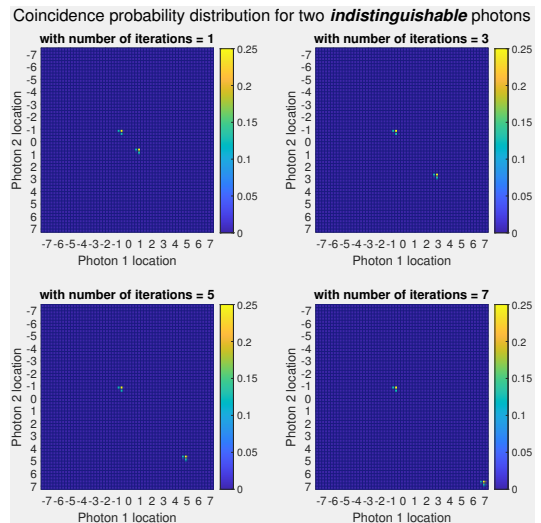

FIG. 6: The spatial distribution of the photon amplitudes for two photons at four different times, given an initial state with two *indistinguishable* photons entering ports one and two of the four-port at position $m = 0$. The two axes give the locations of the two photons, labelled by the integer-valued four-port index. It is seen that the amplitude splits into two localized components, but that the two photons are always found clustered together within the *same* component, as indicated by the absence of amplitude away from the descending diagonal.
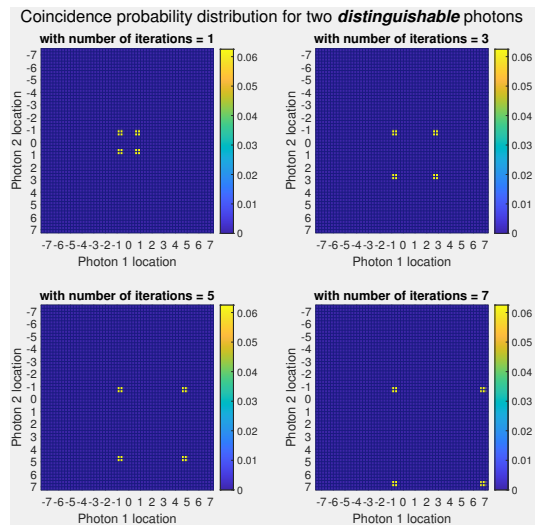

FIG. 7: The spatial distribution of the photon amplitudes for two *distinguishable* photons. In contrast to the indistinguishable case, off-diagonal terms appear, indicating that the two photons no longer remain clustered together.

Analogous to previous sections, focus on the initial state $|\psi_0\rangle_{in} = |A_+^{12}, m\rangle$. (Additional analysis of the A and B states, along with a third set of polarization-entangled states is given in Appendix B.) The output of the first

step is

$$
\begin{aligned}
|\psi_0\rangle_{out} &= \frac{1}{2} \left(\, |A_+^{12}, m, L\rangle + |A_+^{34}, m, R\rangle \right. \\
&\left. \quad + |B_+^{34}, m, R\rangle - |B_+^{12}, m, L\rangle \, \right)_{out}.
\end{aligned}
\tag{22}
$$

It is readily seen that once again the photons cluster: both exit left (ports 1 and 2) or both exit right (3 and 4). *Crucially for entanglement, the two photons are always at different ports: one exits onto the upper line and one onto the lower line.*

This state enters adjacent multiports at the next step as

$$
\begin{aligned}
|\psi_1\rangle_{in} &= \frac{1}{2} \left(|A_+^{34}, m-1, LL\rangle + |A_+^{12}, m+1, RR\rangle \right. \\
&\left. \quad + |B_+^{12}, m+1, RR\rangle - |B_+^{34}, m-1, LL\rangle \right)_{in},
\end{aligned}
\tag{23}
$$

$$
= \frac{1}{\sqrt{2}} \left(|\psi_r, m-1, LL\rangle + |\psi_t, m+1, RR\rangle \right),
\tag{24}
$$

where

$$
|\psi_r\rangle \equiv \frac{1}{\sqrt{2}} \left(|A_+^{34}\rangle - |B_+^{34}\rangle \right)
\tag{25}
$$

and

$$
|\psi_t\rangle \equiv \frac{1}{\sqrt{2}} \left(|A_+^{12}\rangle + |B_+^{12}\rangle \right).
\tag{26}
$$

[Similarly, if the input state had been $|B_+^{12}, m\rangle$, the resulting output would have been $\frac{1}{\sqrt{2}} \left(|\psi_r, m-1, LL\rangle - |\psi_t, m+1, RR\rangle \right)$.] Calculations similar to the previous section show these again to be totally transmitting and totally reflecting: $|\psi_r\rangle$ subsequently oscillates back and forth near the origin, while $|\psi_t\rangle$ remains unchanged aside from repeatedly shifting rightward by one step per unit time. So the picture remains the same as in the previous section, but with the additional feature that *the polarization-entanglement remains undiminished as the walk proceeds.* Which polarization is on which edge is indeterminate until measured, and clustered two-photon states remain polarization-entangled between upper and lower edges as they propagate. Perfect state transport (PST) occurs probabilistically (50% probability) for $|\psi_t\rangle$, delivering two entangled photons to the same horizontal location at the same time.

V. COHERENT STATE INPUT

It is natural to ask how other types of states propagate through this system. Consider, for example, coherent state input. In particular, consider the state

$$
|\psi_{in}\rangle = |\alpha\rangle_1 |\alpha\rangle_2 |0\rangle_3 |0\rangle_4
\tag{27}
$$

with equal amplitude coherent states entering ports 1 and 2 at some lattice site (here we omit directional and site

labels again to streamline notation). This state can be written in terms of displaced vacuum states as

$$
\begin{aligned}
|\psi_{in}\rangle &= e^{-\frac{1}{2}|\alpha|^2} e^{\alpha \hat{a}_1^\dagger - \alpha^* \hat{a}_1} e^{-\frac{1}{2}|\alpha|^2} \\
&\quad \times e^{\alpha \hat{a}_2^\dagger - \alpha^* \hat{a}_2} |0\rangle_1 |0\rangle_2 |0\rangle_3 |0\rangle_4.
\end{aligned}
\tag{28}
$$

After passage through the four-port, the output state is

$$
\begin{aligned}
|\psi_{out}\rangle &= e^{-\frac{1}{2}|\alpha|^2} e^{\frac{1}{2}\alpha(-\hat{a}_1^\dagger + \hat{a}_2^\dagger + \hat{a}_3^\dagger \hat{a}_4^\dagger)} e^{-\alpha^*(-\hat{a}_1 + \hat{a}_2 + \hat{a}_3 + \hat{a}_4)} \\
&\quad \times e^{-\frac{1}{2}|\alpha|^2} e^{\frac{1}{2}\alpha(\hat{a}_1^\dagger - \hat{a}_2^\dagger + \hat{a}_3^\dagger + \hat{a}_4^\dagger)} \\
&\quad \times e^{-\alpha^*(\hat{a}_1 - \hat{a}_2 + \hat{a}_3 + \hat{a}_4)} |0\rangle_1 |0\rangle_2 |0\rangle_3 |0\rangle_4
\end{aligned}
\tag{29}
$$

$$
= e^{-|\alpha|^2} e^{\alpha(\hat{a}_3^\dagger + \hat{a}_4^\dagger) - \alpha^*(\hat{a}_3 + \hat{a}_4)} |0\rangle_1 |0\rangle_2 |0\rangle_3 |0\rangle_4
\tag{30}
$$

$$
= |0\rangle_1 |0\rangle_2 |\alpha\rangle_3 |\alpha\rangle_4.
\tag{31}
$$

Iterating the process, it is clear that this balanced double coherent state propagates indefinitely without reflection.

The unidirectional propagation follows from the fact that the amount of amplitude reflected backward along line 1 (for example) contains equal contributions from the light that had entered at ports 1 and 2, but these two amplitudes will reflect out port 1 with opposite sign. Equivalently, the Grover four-port selects out only the portion of the reflected state that is antisymmetric under interchange of upper and lower lines, but the input contained only a symmetric part.

Coherent state amplitudes are inherently fluctuating objects, so arranging equal amplitudes in the two lines over multiple steps may seem unlikely. It is therefore sensible to look at what happens when the input coherent states are unbalanced, with amplitude α in the upper line and amplitude β in the lower line:

$$
|\psi_{in}\rangle = |\alpha\rangle_1 |\beta\rangle_2 |0\rangle_3 |0\rangle_4.
\tag{32}
$$

Manipulations along the same lines as above lead after one step through the Grover four-port to the output

$$
|\psi_{out}\rangle = |\frac{\beta - \alpha}{2}\rangle_1 |\frac{\alpha - \beta}{2}\rangle_2 |\frac{\alpha + \beta}{2}\rangle_3 |\frac{\alpha + \beta}{2}\rangle_4.
\tag{33}
$$

There is now both rightward transmission and leftward reflection; however notice that the amplitudes on the two right-moving lines are of equal amplitude again. Thus, any fluctuations in the input amplitude on the left are automatically evened out in the rightward traveling transmitted amplitudes. This is again due to the fact that the two rightward amplitudes are each equal superpositions of the two input modes, so any fluctuation in one input is equally shared between the two outputs. If measurements are made at some point N steps to the right of the input, the output arriving at a given time is guaranteed to have equal amplitudes in both lines, regardless of reflections or losses, or of initially unequal inputs. A similar conclusion will hold for output measured at some distance to the *left* of the initial point.

VI. CONCLUSIONS

We have shown that two-particle quantum interference allows two non-interacting, indistinguishable walkers to remain clustered as they walk along a chain of directionally-unbiased Grover four-ports. The resulting state is a superposition of two spatially-localized two-photon clusters, one confined near the origin, the other moving monotonically away. If the particles are entangled, the pair moves as a single unit, with undiminished entanglement. Whereas perfect state transport has been demonstrated for single photon states in various systems [36–38], this system demonstrates the existence of PST for entangled multi-particle states as well, with 50% arrival probability.

Potential applications are readily envisioned. Entangled pairs can be delivered in a controllable manner to distant locations for standard applications like entanglement swapping, quantum repeaters, or to control the flow of entanglement for two-photon interference effects in quantum networks [39]. Since the ballistic part moves with constant speed, these locations are addressable simply by waiting the appropriate amount of time for the amplitude to arrive. Similarly, new communication or quantum key distribution protocols can be imagined requiring two spatially-separated participants to simultaneously share equal access to the amplitudes of both photons in an entangled pair; the presence of two photons in each spatially-separated state ($|\psi_t\rangle$ and $|\psi_r\rangle$) could be used for error detection, for example.

One reason why utilizing the clustering effect can be useful in such applications, rather than simply sending a photon pair along a fiber or through free space, is that by adding phase shifts in the lines between the multiports the flow of the photon pairs can be controlled; they can be stopped at a desired location (oscillating between two adjacent multiports) or their direction of motion can be reversed. This sort of control is something that can't by done with a simple optical fiber, and here it can be done without damaging any entanglement between the photons. The means of such control is readily seen: inserting phase shifts of $\frac{\pi}{2}$ to an upper line and $-\frac{\pi}{2}$ to the corresponding lower line converts the reflecting and transmitting states of Eqs. 13 and 14 into each other, allowing the experimenter to controllably switch back and forth between ballistic and oscillating behavior.

Furthermore, the fact that there are two spatially-separated two-photon amplitudes means that those amplitudes can be brought back together and interfered with each other. This provides a means of probing the region that the ballistic portion has traveled through, allowing new two-photon sensing methods. For example, if one photon is vertically-polarized and one horizontally-polarized (the entangled $|A_+^{12}\rangle$ state, for instance), they may gain different polarization-dependent phase shifts due to external magnetic fields; even very small relative phase shifts will destroy the clustering effect, leading to a dip in the two-photon interference (similar to the Hong-Ou-Mandel dip) when the two halves of the superposition are brought back together, allowing sensitive detection of external fields in the relevant region.

In addition, the results of the previous section show that this arrangement can be used to correct for differential losses between pairs of coherent state beams. This is a significant benefit in coherent state interference experiments.

Applications and further properties of this system will be examined in detail elsewhere.

Appendix A: Calculation of Output Probabilities

Here, for reference, additional details of the calculations used in the main text are filled in. We work in the basis $\{|1\rangle, |2\rangle, |3\rangle, |4\rangle\}$, where $|n\rangle$ represents a photon in port n. We suppress directional labels when the direction (ingoing or outgoing from the multiport) is clear, as well as dropping site labels when they are not needed. A single photon state entering or exiting a given multiport can be written as a column matrix:

$$\begin{pmatrix} a \\ b \\ c \\ d \end{pmatrix} = a|1\rangle + b|2\rangle + c|3\rangle + d|4\rangle. \quad (A1)$$

The matrix U of Eq. 1 then acts on such column matrices.

For input state $|1\rangle$, transition matrix U then gives output

$$|1\rangle \rightarrow \left(\frac{1}{2}\right)(-|1\rangle + |2\rangle + |3\rangle + |4\rangle); \quad (A2)$$

the action on input states $|2\rangle$, $|3\rangle$, $|4\rangle$ are just cyclical permutations of this.

The action on two-particle input states is obtained by taking products of two single particle output states. For example, given a two-photon input state $|12\rangle = |1\rangle|2\rangle$, with one photon entering port 1 and one photon entering
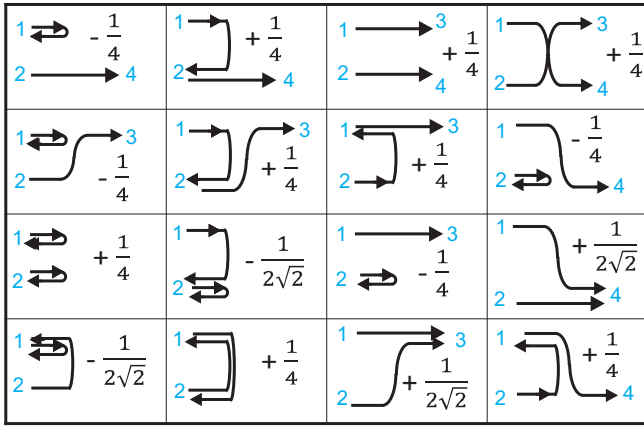
FIG. 8: Amplitudes for all the two-particle paths through a single four-port.

port 2, the output is of the form:

$$|12\rangle \; \rightarrow \; \frac{1}{4}\left(-|1\rangle + |2\rangle + |3\rangle + |4\rangle\right) \tag{A3}$$

$$\cdot\left(+|1\rangle - |2\rangle + |3\rangle + |4\rangle\right)$$

$$= \; \frac{1}{4}\left(-|11\rangle + |12\rangle - |13\rangle - |14\rangle\right) \tag{A4}$$

$$+|21\rangle - |22\rangle + |23\rangle + |24\rangle$$

$$+|31\rangle - |32\rangle + |33\rangle + |34\rangle$$

$$+|41\rangle - |42\rangle + |43\rangle + |44\rangle)$$

$$= \; \frac{1}{4}\left(-|11\rangle + 2|12\rangle - |22\rangle + |33\rangle + |44\rangle + 2|34\rangle\right)$$

$$= \; \frac{1}{4}\left(-\sqrt{2}|2,0,0,0\rangle + 2|12\rangle - \sqrt{2}|0,2,0,0\rangle\right. \tag{A5}$$

$$\left. +\sqrt{2}|0020\rangle + \sqrt{2}|0002\rangle + 2|34\rangle\right),$$

where, for example, $|2,0,0,0\rangle$ represents the Fock state with two-photons in port 1, and zero photons in ports 2, 3, and 4. The extra factors of $\sqrt{2}$ in the last line come from writing the states with two photons in the *same* port in terms of the two-particle Fock state in port n with standard normalization; for example,

$$|11\rangle = a^\dagger a^\dagger |0\rangle = \sqrt{2}|2,0,0,0\rangle. \tag{A6}$$

The transitions amplitudes from initial input state

$$|\psi_0\rangle = |12\rangle \tag{A7}$$

to all possible output states are then easy to tabulate and are shown in the table of Fig. 8.

Exit probabilities can be found by adding the amplitudes for indistinguishable outcomes and squaring. For example, the probability for the photons to exit at ports 3 and 4 is given by the squared sum of two amplitudes (Fig. 9):

$$P(|\psi_0\rangle \rightarrow |34\rangle) = \frac{1}{2}\left(\frac{1}{2\sqrt{2}} + \frac{1}{2\sqrt{2}}\right)^2 = \frac{1}{4}.$$
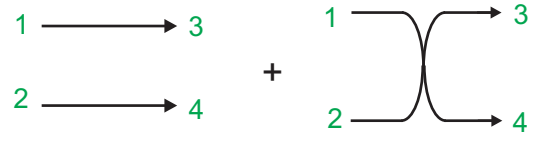

FIG. 9: Amplitudes of indistinguishable outcomes must be added; shown here the amplitudes for exit at ports 3 and 4 (the two cells in the top right corner of Fig. 8), which add and then square to give the probability $P(|\psi_0\rangle \rightarrow |34\rangle)$ in Table I.

Transition	Probability	Exit Direction
$|\psi_0\rangle \rightarrow |11\rangle$	$P = \left(-\frac{1}{2\sqrt{2}}\right)^2 = \frac{1}{8}$	LL
$|\psi_0\rangle \rightarrow |12\rangle$	$P = \left(\frac{1}{4} + \frac{1}{4}\right)^2 = \frac{1}{4}$	LL
$|\psi_0\rangle \rightarrow |13\rangle$	$P = \left(\frac{1}{4} - \frac{1}{4}\right)^2 = 0$	LR
$|\psi_0\rangle \rightarrow |14\rangle$	$P = \left(\frac{1}{4} - \frac{1}{4}\right)^2 = 0$	LR
$|\psi_0\rangle \rightarrow |22\rangle$	$P = \left(-\frac{1}{2\sqrt{2}}\right)^2 = \frac{1}{8}$	LL
$|\psi_0\rangle \rightarrow |23\rangle$	$P = \left(\frac{1}{4} - \frac{1}{4}\right)^2 = 0$	LR
$|\psi_0\rangle \rightarrow |24\rangle$	$P = \left(\frac{1}{4} - \frac{1}{4}\right)^2 = 0$	LR
$|\psi_0\rangle \rightarrow |33\rangle$	$P = \left(+\frac{1}{2\sqrt{2}}\right)^2 = \frac{1}{8}$	RR
$|\psi_0\rangle \rightarrow |34\rangle$	$P = \left(\frac{1}{4} + \frac{1}{4}\right)^2 = \frac{1}{4}$	RR
$|\psi_0\rangle \rightarrow |44\rangle$	$P = \left(+\frac{1}{2\sqrt{2}}\right)^2 = \frac{1}{8}$	RR

TABLE I: Two-photon exit probabilities for input $|\psi_0\rangle$.

Table I lists the amplitudes for all possible output states of the Grover coin four-port, assuming input state $|\psi_0\rangle$.

The probabilities of both photons exiting left, both right, or of one in each direction are then found by simply adding the probabilities from the table,

$$P(\psi_0 \rightarrow LL) \; = \; \frac{1}{8} + \frac{1}{4} + \frac{1}{8} = \frac{1}{2} \tag{A8}$$

$$P(\psi_0 \rightarrow RR) \; = \; \frac{1}{8} + \frac{1}{4} + \frac{1}{8} = \frac{1}{2} \tag{A9}$$

$$P(\psi_0 \rightarrow LR) \; = \; 0, \tag{A10}$$

as claimed in the main text (Eqs. 6-10).

Appendix B: Action of Grover Coin on Entangled States

First, recall the standard maximally-entangled Bell states:

$$|\Psi^\pm\rangle \; = \; \frac{1}{\sqrt{2}}\left(|1H\rangle|2V\rangle \pm |1V\rangle|2H\rangle\right) \tag{B1}$$

$$|\Phi^\pm\rangle \; = \; \frac{1}{\sqrt{2}}\left(|1H\rangle|2H\rangle \pm |1V\rangle|2V\rangle\right), \tag{B2}$$

where, for example, $|jH\rangle$ represents a horizontally polarized photon in port j.

Then define an additional set of states:

$$|A^{ij}_\pm\rangle = \frac{1}{\sqrt{2}}\left(|iH\rangle|jV\rangle \pm |iV\rangle|jH\rangle\right) \quad \text{(B3)}$$

$$|B^{ij}_\pm\rangle = \frac{1}{\sqrt{2}}\left(|iH\rangle|iV\rangle \pm |jV\rangle|jH\rangle\right) \quad \text{(B4)}$$

$$|C^{ij}_\pm\rangle = \frac{1}{\sqrt{2}}\left(|iH\rangle|jH\rangle \pm |iV\rangle|jV\rangle\right). \quad \text{(B5)}$$

These have the following properties:

• If $i = j$: $|A^{jj}_+\rangle = |B^{jj}_+\rangle$, and $|A^{jj}_-\rangle = |B^{jj}_-\rangle = 0$.

• For $i \neq j$, $|C^{12}_\pm\rangle = |\Phi^\pm\rangle$, $|A^{12}_\pm\rangle = |\Psi^\pm\rangle$ are maximally entangled Bell states.

• $|C^{11}_\pm\rangle$ and $|C^{11}_\pm\rangle$ can be seen as $N00N$ states with $N = 2$ polarized photons.

We now examine how these states behave under the action of the Grover four-port, and see for which initial states two-photon clustering occurs.

I. The A^{12}_+ state is already studied in Section IV. We know that at the first step it splits into a *sum* of reflecting and transmitting states:

$$|A^{12}_+\rangle \to |\psi_t\rangle + |\psi_r\rangle. \quad \text{(B6)}$$

The two photons in the reflecting and transmitting states then continue to cluster in all subsequent steps.

II. In a similar manner, B^{12}_+ splits into a *difference* of reflecting and transmitting states:

$$|B^{12}_+\rangle \to |\psi_t\rangle - |\psi_r\rangle, \quad \text{(B7)}$$

again leading to photon clustering.

III. The product state $A^{11}_+ = \sqrt{2}|1H\rangle|1V\rangle$ transforms under the Grover coin at the first step as

$$|A^{11}_+\rangle \to \frac{1}{2\sqrt{2}}\big[|1H\rangle|1V\rangle + |2H\rangle|2V\rangle \quad \text{(B8)}$$
$$+ |3H\rangle|3V\rangle + |4H\rangle|4V\rangle$$
$$- (|1H\rangle|2V\rangle + |2H\rangle|1V\rangle)$$
$$- (|1H\rangle|3V\rangle + |3H\rangle|1V\rangle)$$
$$- (|1H\rangle|4V\rangle + |4H\rangle|1V\rangle)$$
$$+ (|2H\rangle|3V\rangle + |3H\rangle|2V\rangle)$$
$$+ (|2H\rangle|4V\rangle + |4H\rangle|2V\rangle)$$
$$+ (|3H\rangle|4V\rangle + |4H\rangle|3V\rangle)\big].$$

Since cross terms occur that mix left-moving (1 and 2) exit states with right-moving (3 and 4) states, no clustering occurs. $|A^{22}_+\rangle$ behaves similarly.

IV. A^{12}_- input leads to output at the first step of the form:

$$|A^{12}_-\rangle \to \frac{1}{2\sqrt{2}}\big[(|1V\rangle|4H\rangle - |1H\rangle|4V\rangle) \quad \text{(B9)}$$
$$+ (|1V\rangle|3H\rangle - |1H\rangle|3V\rangle)$$
$$+ (|2H\rangle|3V\rangle - |3H\rangle|2V\rangle)$$
$$+ (|2H\rangle|4V\rangle - |2V\rangle|4H\rangle)\big].$$

Not only does clustering not occur, but the two photons always go in *opposite* directions at this first step. (This repulsion of course does not continue on subsequent steps, since the interference no longer occurs once the photons are separated.)

V. The $C^\pm_{11}$ states transform at the first step as follows:

$$|C^{11}_\pm\rangle \to \frac{1}{4\sqrt{2}}\big(|1H\rangle|1H\rangle + |2H\rangle|2H\rangle \quad \text{(B10)}$$
$$+ |3H\rangle|3H\rangle + |4H\rangle|4H\rangle\big)$$
$$+ \frac{1}{2\sqrt{2}}\big[(|2H\rangle|3H\rangle + |2H\rangle|4H\rangle + |3H\rangle|4H\rangle)$$
$$- (|1H\rangle|2H\rangle + |1H\rangle|3H\rangle + |1H\rangle|4H\rangle)\big]$$
$$\pm \text{ same with } H \to V.$$

This does not cluster because of the crossed terms mixing 1 and 2 with 3 and 4 in the second line. $C^\pm_{22}$ behaves in a similar manner.

VI. $C^{12}_\pm$ becomes a linear combination of all of the C states under the action of the four-port:

$$|C^{12}_\pm\rangle \to \frac{1}{4}\left(-|C^{11}_\mp\rangle - |C^{22}_\mp\rangle + |C^{33}_\pm\rangle + |C^{44}_\pm\rangle\right)$$
$$+ \frac{1}{4}\left(|C^{12}_\pm\rangle + |C^{34}_\pm\rangle\right). \quad \text{(B11)}$$

In subsequent steps, this state then declusters because the $C^{jj}_\pm$ states in the first parentheses decluster, as shown in IV above.

So, summarizing, the A^{12}_+ and B^{12}_+ states will always cluster, while the remainder of the A, B, and C states will not.

---

[1] C. K. Hong, Z. Y. Ou, L. Mandel, Phys. Rev. Lett. **59**, 2044 (1987)
[2] A. M. Childs, Phys. Rev. Lett. **102**, 180501 (2009).
[3] N. B. Lovett, S. Cooper, M. Everitt, M. Trevers, V. Kendon, Phys. Rev. A. **81**, 042330 (2010).
[4] R. Portugal, *Quantum Walks and Search Algorithms* (Springer, 2013).
[5] J. Kempe, Contemp. Phys. **44**, 307 (2003).
[6] A. Ambainis, Int. J. Quantum Inf. **1**, 507 (2003).
[7] A. Ambainis, E. Bach, A. Nayak, A. Vishwanath, and

J. Watrous, in Proceedings of the Thirty-third Annual ACM Symposium on Theory of Computing (STOC '01), ACM, New York, NY, USA, 37 (2001) .

[8] L. K. Grover, A fast quantum mechanical algorithm for database search, in Proceedings of the Twenty-Eighth Annual ACM Symposium on the Theory of Computing, pages 212-219, Philadelphia, Pennsylvania, 22-24 May 1996.

[9] N. Shenvi, J. Kempe, R. B. Whaley, A quantum random walk search algorithm. Phys. Rev. A 67(5), 052307 (2003).

[10] Y. Omar, N. Paunković, L. Sheridan, and S. Bose, Phys. Rev. A **74**, 042304 (2006).

[11] P. K. Pathak and G. S. Agarwal, Phys. Rev. A **75**, 032351 (2007).

[12] S.-Y. Shiau, R. Joynt, and S. Coppersmith, Quantum Inf. Comput. **5**, 492 (2005).

[13] J. K. Gamble, M. Friesen, D. Zhou, R. Joynt, and S. N. Coppersmith, Phys. Rev. A **81**, 052313 (2010).

[14] F. Zähringer, G. Kirchmair, R. Gerritsma, E. Solano, R. Blatt, and C. F. Roos, Phys. Rev. Lett. **104**, 100503 (2010).

[15] A. Peruzzo et al., Science **329**, 1500 (2010).

[16] M. Štefaňák, T. Kiss, I. Jex, and B. Mohring, J. Phys. A **39**, 14965 (2006).

[17] P. P. Rohde, A. Schreiber, M. Štefaňák, I. Jex, and C. Silberhorn, New J. Phys. **13**, 013001 (2011).

[18] S. D. Berry and J. B. Wang, Phys. Rev. A **83**, 042317 (2011).

[19] G. R. Carson, T. Loke, J. B. Wang, Quant. Inf. Process. **14**, 3193 (2015).

[20] S. Fan, P. R. Villeneuve, J. D. Joannopoulos, H. A. Haus, Phys. Rev. Lett. **80**, 960 (1998).

[21] G. M. Nikopoulos, Phys. Rev. Lett. **101**, 200502 (2008).

[22] D. S. Simon, C. A. Fitzpatrick and A. V. Sergienko, Phys. Rev. A **93**, 043845 (2016).

[23] D. S. Simon, C. A. Fitzpatrick, S. Osawa, and A. V. Sergienko, Phys. Rev. A **95**, 042109 (2017).

[24] D.S. Simon, C. A. Fitzpatrick, S. Osawa, and A.V. Sergienko, Phys. Rev. A **96**, 013858 (2017).

[25] D. S. Simon, S. Osawa, A. V. Sergienko, New J. of Phys. **20**, 093032 (2018).

[26] S. Osawa, D. S. Simon, A.V. Sergienko, Opt. Expr. **26**, 27201 (2018).

[27] S. Osawa, D. S. Simon, A.V. Sergienko, Entropy **21**, 853 (2019).

[28] L. Sansoni, F. Sciarrino, G. Vallone, P. Mataloni, A. Crespi, R. Ramponi, and R. Osellame, Phys. Rev. Lett. **108**, 010502 (2012).

[29] Q. P. Su, Y. Zhang, L. Yu, J. Q. Zhou, J. S. Jin, X. Q. Xu, S. J. Xiong, Q. J. Xu, Z. Sun, K. Chen, F. Nori, and C. P. Yang, npj Quantum Information, **5**, Article number 40 (2019).

[30] A. Crespi, R. Osellame, R. Ramponi, V. Giovannetti, R. Fazio, L. Sansoni, F. De Nicola, F. Sciarrino, and P. Mataloni, Nature Photonics **7**, 322 (2013).

[31] A. Geraldi, L. D. Bonavena, C. Liorni, P. Mataloni, A. Cuevas, Condens. Matter **4**, 14 (2009).

[32] C. Moore and A. Russell, in Proc. 6th Intl. Workshop on Randomization and Approximation Techniques in Computer Science (RANDOM 02), p. 164, J. D. P. Rolim and S. Vadhan eds. (Springer, 2002).

[33] I. Carneiro, M. Loo, X. Xu, M. Girerd, V. Kendon, P. L. Knight, New J. Phys. **7**, 156 (2005).

[34] R. Boyd, *Nonlinear Optics, 3rd ed.* (Academic Press, NY, 2008).

[35] A. Ambainis, K. Prüsis, J. Vihrovs, T. G. Wong, Phys. Rev. A **94** 062324 (2016).

[36] M. Bellec, G. M. Nikolopoulos, S. Tzortzakis, Opt. Lett. **37**, 4504 (2012).

[37] A. Perez-Leija, R. Keil, A. Kay, H. Moya-Cessa, S. Nolte, L. C. Kwek, B. M. Rodriguez-Lara, A. Szameit, D. N. Christodoulides, Phys. Rev. A **87**, 012309 (2013).

[38] R.J. Chapman, M. Santandrea, Z. Huang, G. Corrielli, A. Crespi, M.-H. Yung, R. Osellame, A. Peruzzo, Nat. Comm. **7** (2016).

[39] A. R. McMillan, et. al., Sci. Rep. **3**, 2032 (2013).